

Received April 21, 2021, accepted April 26, 2021, date of publication April 29, 2021, date of current version May 19, 2021.

Digital Object Identifier 10.1109/ACCESS.2021.3076484

# On-The-Move Measurement Analysis for Ka-Band High Throughput Satellite and LiFi Communication Networks in Tropical Region

P. M. KALAIVAANAN<sup>1</sup>, (Graduate Student Member, IEEE), ADUWATI SALI<sup>1</sup>, (Senior Member, IEEE), RAJA SYAMSUL AZMIR RAJA ABDULLAH<sup>1</sup>, (Senior Member, IEEE), SYAMSURI YAAKOB<sup>1</sup>, (Senior Member, IEEE), MANDEEP JIT SINGH<sup>2,3</sup>, AND ALI M. AL-SAEGH<sup>4</sup>

<sup>1</sup>Fakulti Kejuruteraan, Universiti Putra Malaysia, Serdang 43400, Malaysia

<sup>2</sup>Department of Electrical, Electronic and Systems Engineering, Faculty of Engineering and Built Environment, Universiti Kebangsaan Malaysia, Bangi 43600, Malaysia

<sup>3</sup>Space Science Centre (ANGKASA), Institute of Climate Change, Universiti Kebangsaan Malaysia, Bangi 43600, Malaysia

<sup>4</sup>Al-Ma'moon University College, Communications Engineering College, Baghdad 100001, Iraq

Corresponding authors: P. M. Kalaivaanan (gs52374@student.upm.edu.my) and Aduwati Sali (aduwati@upm.edu.my)

This work was supported by the EMOSEN—Energy Efficient MIMO-Based Wireless Transmission (SWIPT—Enabled Network) for technical and resource support with signed mutual non-disclosure agreement (NDA) with ERL under Grant UPM/800-3/3/1/GPB/2019/9671600.

**ABSTRACT** With the point in evaluating the performance of the On-the-Move (OTM) Satellite Communication and Light Fidelity (SatCom-LiFi), an extensive study of measurement has been conducted to give a wide vision of the SatCom-LiFi potential under a tropical region. As the interest for OTM network connectivity to offload the C-band capacity arises due to frequency spectrum scarcity, satellite networks offer to balance topographical requirements under tropical environment as the Next Generation Networks (NGN) trend for OTM communication system solutions. To date, mobile satellite terminal propagation model was carried out at temperate regions where further experimental measurement is needed under the OTM scenario in tropical region. This paper discusses on the areas where there are limited real-time data under the OTM scenario (e.g. rain attenuation, power arch) at Ka-band frequency. Integration infers, to be specific, the use of new elements capable in providing performance analysis of all systems involved and to take possible decision, in determining the need for a technically feasible solution. Measurement results reveal that, throughput data rate of 15 Mbps were able to be delivered for more than 80% of the time under the speed of 150 km/h with shielded mesh antenna. In addition to that, this paper reveals the favorable circumstances and inadequacies of OTM network quality, in which the measurement presented plays an important role for future researchers in distinguishing highly accurate predictions.

**INDEX TERMS** OTM, HTS, SatCom-LiFi, Ka-band satellite communication.

## I. INTRODUCTION

It is imperative to comment that these days where SatCom-LiFi does not fulfill the full set of solution/technology criteria under tropical region. With the demand of anticipated broadband access capacity, big data and stringent requirement for OTM application shall be established [1], [2]. Focusing on these two heterogeneous

The associate editor coordinating the review of this manuscript and approving it for publication was Shah Nawaz Burokur<sup>1</sup>.

network communication architectures, more challenging criteria fall under the high-speed rail (HSR) communication solution. High Throughput Satellite (HTS) solutions become technically feasible for last mile client device to handshake with the throughput between SatCom and LiFi network. Latest invented optical LiFi communication technology offers high data rate (3 ~ 4Gbps) for commercial communication application [3].

Concentrating on these hybrid network communication design, technical feasibility investigation is made under the

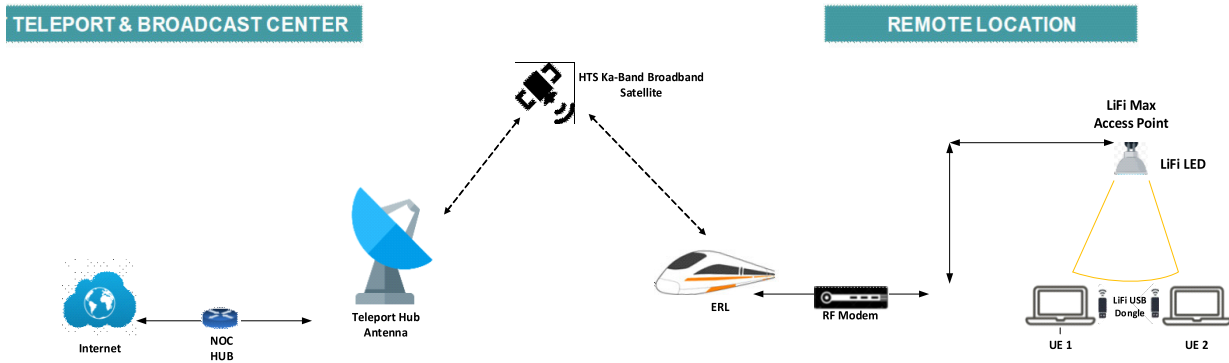


FIGURE 1. Heterogeneous apparatus network connectivity.

clear sky and rainy conditions including measurement of physical constraints (e.g power arch) to determine the network performance, parameter utilization data rate, packet loss and latency [2]–[4].

The primary contribution of the paper can be outlined as follows:

- Measurement analysis of network performance are being carried out in order to improve the network utilization. For the purpose of facilitating the network throughput analysis in tropical region. Under the OTM performance, a heterogeneous hybrid network broadband over HTS via Ka-band and LiFi system are being analysed and validated. To the best of our knowledge, OTM analysis measurement under tropical region are currently limited and to fill this gap, this paper focuses real time measurement and analysis.
- Reference towards SatCom-LiFi network broadband service under the tropical area with various weather conditions and varying scenarios (e.g. clear sky, rainy, power arch and etc.). Several historical attempts (Tropical-Land Mobile Satellite Channel) [5] were presented under Ku-band application to provide complete solution architecture in improving the overall link availability under tropical region [6]–[8].
- Measurement of the actual network response time (network latency and packet loss) for a broadband activity that require minimal delay such as fast paced online-gaming under the OTM system [9].
- Faster implementation of HTS application compared with complex terrestrial network under tropical geographical infrastructure is worth to be analysed (under limited terrestrial coverage area) [10].

Most of the available research paper focuses on a specific channel model (i.e Markov-chain based model) due to absence of direct measurements [5]. For these reasons, the research paper presented real-time measurement analysis campaign to estimate the link performance under the tropical rail condition. The highlight of this paper is to technically evaluate real-time SatCom-LiFi network and its requirement. The future OTM communication architecture is understood to be tailor made with respect to the driver’s critical communication system.

TABLE 1. System setup characteristic.

Subsystem/ Subsystem/ Element	Denotation
NOC HUB	A ISP gateway that handle internet access to the subscriber remote terminal.
Teleport HUB Antenna	RF Interface to access the broadband via radio waves which sends/receives data to/from satellite.
Phase array antenna	Electronically steered to point to the satellite.
GPS antenna	Receive signal for location, velocity and time synchronizer.
SPG	Provides 10MHz reference to RF modem as alternate to outbound satellite carrier
RF modem	A MODEM (MODulator and DEModulator) embeded within the same devices. Hardware that converting digital data into analogue signals typically at IF/L-band
DPI-WAN	Streamline network capacity under Deep packet inspection (DPI) with policy-based technology.
LiFi Max access point & LED	Translating IP network to bits information and vice versa.
User terminal (UE) /USB Dongle	The dongle permits user with secure connection to the internet and moreover used to deliver information backwards to LiFi AP.
Server	To measure the effectiveness of LiFi AP and dongle position before activating the RF transponder

## II. SYSTEM DESCRIPTION

The end-to-end high-level architecture (Figure 1) and the system setup hardware component with complete function are summarized in Table 1. The typical block diagram of the RF component and On-the-Shelf (OTS) LiFi access point (AP) and dongle (LiFiMax®) are shown as per Figure 2 and Figure 3 respectively.

In downlink chain, the RF Ka-band signal modulates at different code rate and received via the array antenna on-top of the rail. The signal is then converted to the intermediate frequency L-band before feeding into the RF modem which then connected to the router with built in deep packet inspection-wide access network (DPI-WAN) software [11], [12]. The network is connected to the LiFi AP with the power over ethernet (PoE) enabled to support power to the LiFi LED [13]. The information bit is then securely established and delivered to the user terminal dongle for active network access.

The duplex communication via HTS, takes reverse part to reach the satellite at different Ka-band frequency,

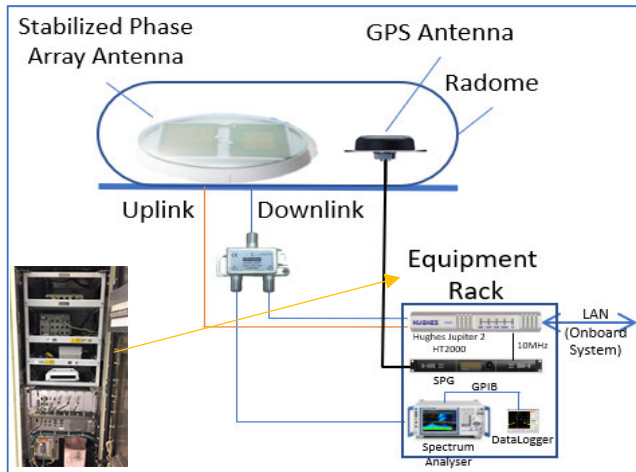


FIGURE 2. SatCom RF connectivity on HSR network.

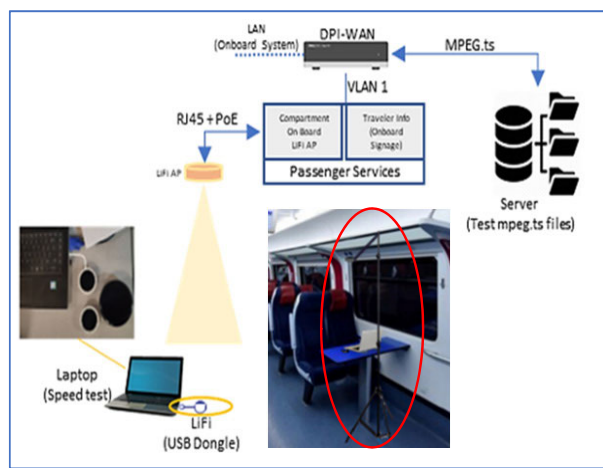


FIGURE 3. Network structure of on-board LiFi network.

polarization and code rate with comparison under the downlink receiving signal. Network signal are then handed over to the teleport to establish secure connection to the internet. Both RF level is implemented in line with link budget calculation to match with real-time results before establishing end to end connection.

### III. MEASUREMENT AND INVESTIGATION

The rain data was collected continuously for past two months (Jan and Feb 2020) at Bukit Jalil and Cyberjaya where analysis is nearest to the track sties. The data was obtained from the locally installed piezoelectric detector sensor from the product of Vaisala RAINCAP<sup>®</sup> sensor technology. For the measurement analysis, array antenna was used and mounted on top of the train. Table 2, represent the antenna and sites specification for the OTM scenario. The downlink chain undergoes several principle functions mainly receiver, filtering, amplification and down conversion which contributed to 2 dB of measured loss.

The minimum mandatory tests with crosspol isolation (CPI) measurement is adequate to guarantee the efficiency deployment of OTM system [6], [14]. CPI minimize

TABLE 2. Antenna, satellite and sites specification.

Measurement Sites	Bukit Jalil	Cyberjaya
Earth Station Location	3.059°N 101.692°E	2.935°N 101.659°E
Beacon Frequency	20.20 GHz (H-pol)	
Satellite	iPStar1 - (119.5°E)	
Antenna Elevation	68.8°	
Antenna Diameter	13.1m	
Antenna, OTM	1.2m	
Ka-band Test Freq.	Tx: 27.46 GHz (V-pol) Rx: 20.02 GHz (H-pol)	
Rain Rate 0.001%	Jan, 2020	137.4 mm/hr
	Feb, 2020	97.8 mm/hr
		101.2 mm/hr
		86.8 mm/hr

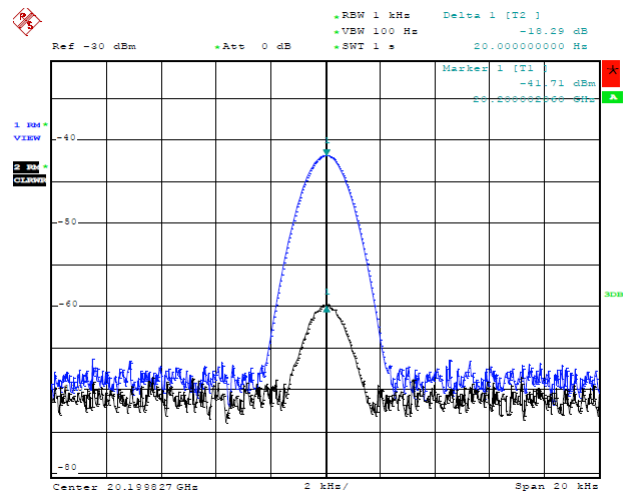


FIGURE 4. Crosspol Isolation measurement of OTM.

interference during uplink by maintaining all potential operational conditions, and to confirm consistence compliance with radio regulations (ITU-R S.580-5) [15]. An extensive set of gain and co-pol measurement have been executed to assess the performance of the array antenna before deploying online. Satellite operator can only approve terminal with lower Cross-Pol Isolation (CPI) values upon conditions of tests results. Based on the CPI measured, > 15 dB isolation achieved, which provide good clearance for transmitting signal (Figure 4) [16], [17].

To benchmark the performance of the array antenna, installation compliance and the beam pointing agility, one-way test (Figure 5) are presented before getting a clearance from both satellite operator and Apparatus Assignment (AA) approval for two-way transmission. The Odin F-50 Forsway modem is connected with receiving downlink from splitter and the 3G/LTE USB dongle as presented in Figure 5.

The sample result for Line of Sight (LoS) situation and clear sky weather condition are captured along the Malaysia Express Rail Link (ERL) route and result of the 3G/LTE are presented in Figure 6 with an average of 0.8Mbps packet sent under the 3G/LTE. Since the track sites are approximately 7 km radius from the analysis area and limited 3G/LTE

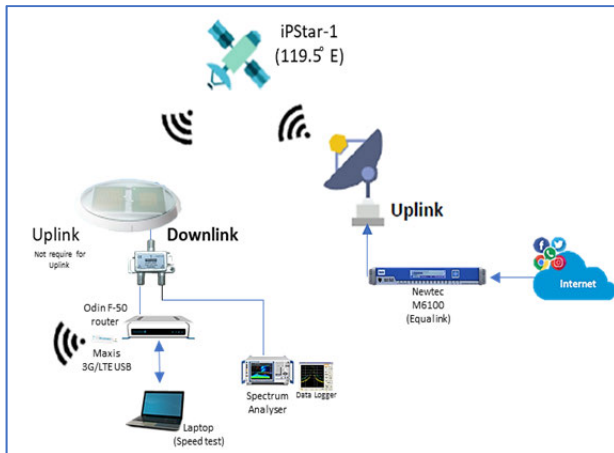


FIGURE 5. One-way connectivity setup.

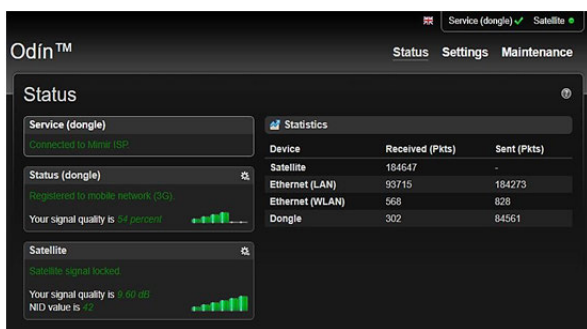


FIGURE 6. Screenshot from modem odin F-50 router webpage.

coverage, the signal strength is recorded as 54%. However, the signal strength is sufficient to verify the antenna pointing agility for one-way test with the result recorded in Table 3.

TABLE 3. One-way connection status.

Measurement	Bukit Jalil	Cyberjaya
Forward (Download)	Ka-band (H-pol) 20.02 GHz	9.6 dB, QPSK 5/6
Return (Upload)	3G/LTE	54%

TABLE 4. Throughput test connection status.

Measurement	C/N	Throughput	PING
With Equalink	9.6 dB	DL:29.97Mbps UL:1.31Mbps	329 ms
Without Equalink	7.1 dB	DL:18.57Mbps UL:1.88Mbps	329 ms

To increase the forward link data throughput, Newtec M6100 modulator with Equalink® linear and non-linear pre-distortion technology were added by the operator [18]. Extra 2 dB link margin has been achieved which improve the overall coverage and increase the symbol rate with lower roll-off factor as result presented in Table 4 and Table 7. By implementing the special features of Equalink®, the

margin and transmission error are well corrected [19] including to compensate the downlink path losses mentioned earlier.

The second stage of setup are focuses on the in-cabin optical communication by using LiFi transceivers (on the shelf LiFiMAX selected for analysis). The analysis focuses on the most important parameter which is *Distance vs. Throughput* at which LiFi communication took place as presented in Figure 3 setup [22]. To achieves a high throughput of LiFi AP and correct position of the setup, 9 different scenarios has been tested with no external lights interference to limit the scope of measurement. In summary, the test characteristic and analysis results are shared in the Table 5 and Table 6 respectively. Table 6 represent the maximum achievable throughput by both of the user 1 and user 2 by comparing with other measurement test scenario. User 1 and 2 represent the passenger siting position in the cabin with the separation denote as  $X_c$  (m) [3].

TABLE 5. LiFi setup characteristics.

Specification	Description
$\theta$ - Angle	Incident angle from the LiFiMAX AP to the user equipment (UE) receiving element
$X_s$ (m)	Separation length between receiving UE to the LiFi AP
$X_r$ (m)	Level between UE with the ERL floor.
$X_c$ (m)	Separation length between two receiving UE

A local LAN network test connection has been performed by using locally stored server/PC in the ERL during the alignment. The laptop and the server are fortified with network ethernet cards: Inter Corporation 82579LM Gigabit Ethernet Controllers. The network interface controller (NICs) support 10/100/1000M speed to ensure a high throughput is supported for LiFi communication [23]–[25].

Line of sight analysis and an optimum position were identified based on the characteristic of LiFi setup as Table 6. This is to ensure a correct position of both the AP and USB dongle is in place for high data rate before connecting to RF network.

TABLE 6. Throughput simulation analysis.

$\theta$ - Angle	$X_s$ (m)	$X_r$ (m)	$X_c$ (m)	Throughput measurement	
				UE 1	UE 2
40°	1.0	0.65	1.0	36.82	35.31
60°	1.0	0.65	1.0	22.41	24.22
90°	1.0	0.65	1.0	11.56	11.23

Table 6, summaries the achieved throughput measurement which is 36.82Mbps and 35.31Mbps at a vertical distance of 1.0m and angle of 40° respectively, since the average vertical distance of sitting position in the ERL are within this range. The small angle (40°) contribute to higher throughput as both UE are concentrated focuses to the LiFiMAX AP. Once both the antenna (1<sup>st</sup> Test) and LiFi optimum (2<sup>nd</sup> Test) position has been identified (based on both of the earlier test), the experimental measurement is extended based on heterogenous SatCom-LiFi integration with inbound and out-bound capability along ERL route.

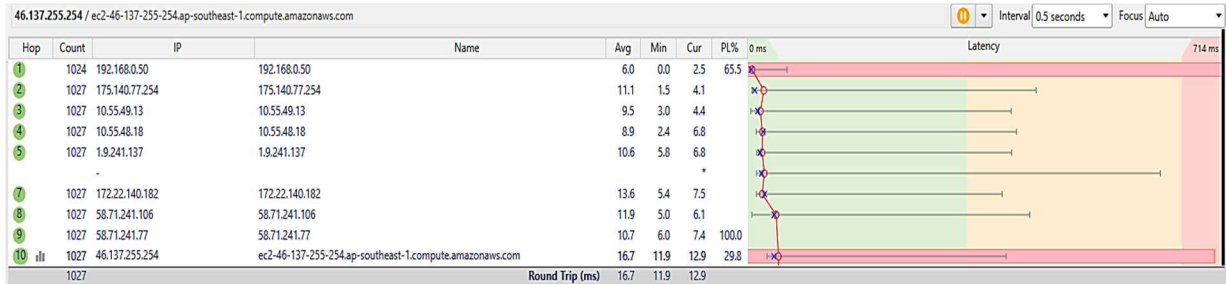


FIGURE 7. Packet loss result for the ERL with constant speed of 150km/h.

TABLE 7. Throughput test connection status.

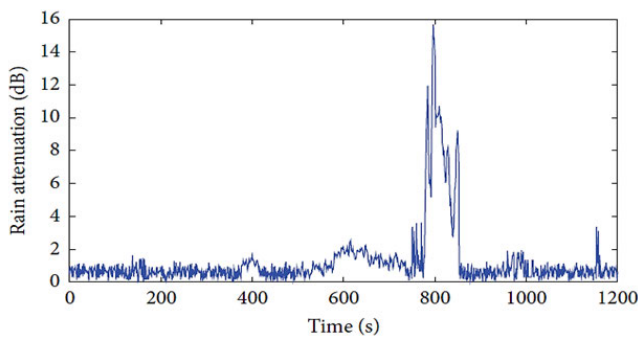


FIGURE 8. Measured rain attenuation during ERL OTP on Feb 14<sup>th</sup>, 2020.

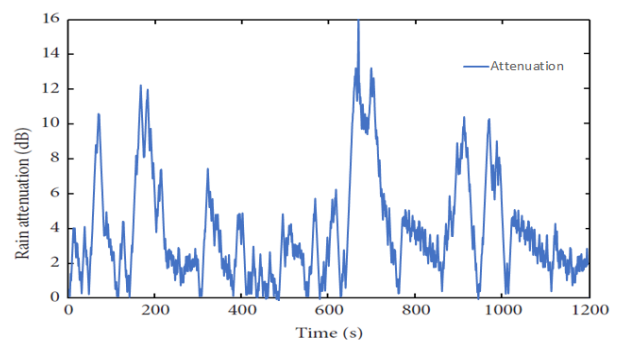


FIGURE 9. Measured rain attenuation during ERL in OTM under the speed of 150km/h on Feb 14<sup>th</sup>, 2020.

The PsTools and PingPlotter is used to measure the handover latency with a recorded of an average of 767ms. Packet loss for both of rainy and clear sky condition [26] were captured and presented in Figure 7.

The measurement set-up basically consists of both transmitter and receiver in the ERL up to the LiFi network and Teleport NOC with both act as forward and return link (Figure 1, Figure 2 and Figure 3). Both outbound and inbound of Adaptive Coding Modulation (ACM) information are

measured during the clear sky to rainy day and ERL is moving with a constant speed of 150km/h [10].

A followed-up on the investigation, the ACM performance can be substantiated [28] in the event of atmospheric fading effects (under rain fading effect commencing the clear sky towards rainy day on Feb 14<sup>th</sup>, 2020).

Each shift in the attenuation (Figure 8, 9 & 10), streamline the link connection modulation and coding

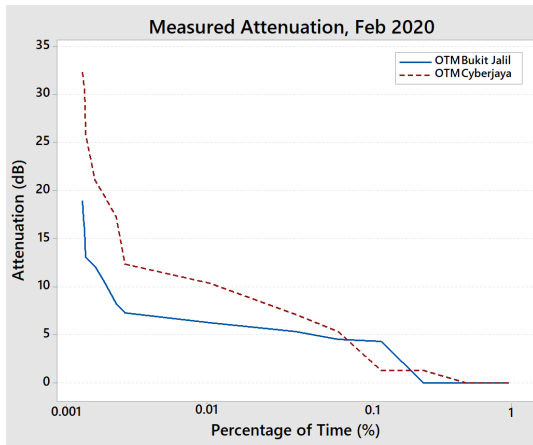


FIGURE 10. Measured rain attenuation along the ERL track sites.

schemes (MODCODs) and affect the total bandwidth, that include the rate limit of a received signal.

To ensure a reliable comparison between OTP and OTM rain attenuation, a 20 minutes analysis duration with a 1 second of sweeping time was performed on Feb, 14<sup>th</sup> 2020 which recorded highest and longest rain rate in the month. Figure 8 represent measured rain attenuation loss in the down-link signal power when the ERL was On-The-Pause (OTP). Whereas, Figure 9 show the measured rain attenuation in the downlink signal when the ERL is OTM. Figure 8, shows the effective rain start from the 10<sup>th</sup> minutes (580 second) and reached to the higher attenuation of 16 dB at minute of 13 (800 second).

However, for the OTM measurement as presented on Figure 9, the attenuation recorded starting from the 1<sup>st</sup> minutes (80 second) until the ERL stops after 20 minutes (1200 second). The downlink beacon level including rain rate were logged every second simultaneously to ensure no missing data for analysis. A cumulative distribution function (CCDF) is plotted (Figure 10) to identify the duration unavailability of RF link for OTM system analysis [28]. The ACM automatically tunes to higher coding and modulation without impacting of the overall network packet and throughput once the link condition improves.

The average precipitation was measured and recorded at two points along the ERL track which is Bukit Jalil (Bj) and Cyberjaya (Cy) which is close to 15 km apart with an elevation angle of 68.8°. An average of rain intensity for 5years from 2016 till 2020 is captured and presented in Figure 11 with the attenuation in Figure 12. It shows that the average rain intensity at 0.01% for Cyberjaya is at 80 mm/h and for Bukit Jalil is at 70 mm/h respectively. The analysis estimation rain intensity in ITU-R P.837 [29] is 90 mm/h and almost to the recorded measurement but not close to the actual on-site measure value. The attenuation at both location experience higher attenuation value with a range of 45 dB to 60 dB as plot presented in Figure 12.

The maximum rain rate of each year from 2016 till 2020 is taken and averaged for the analysis based on the

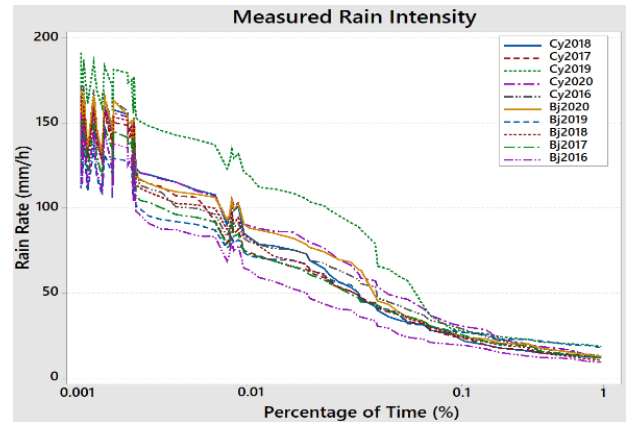


FIGURE 11. Measured rain intensity from 2016 until 2020 for both Cy and Bj.

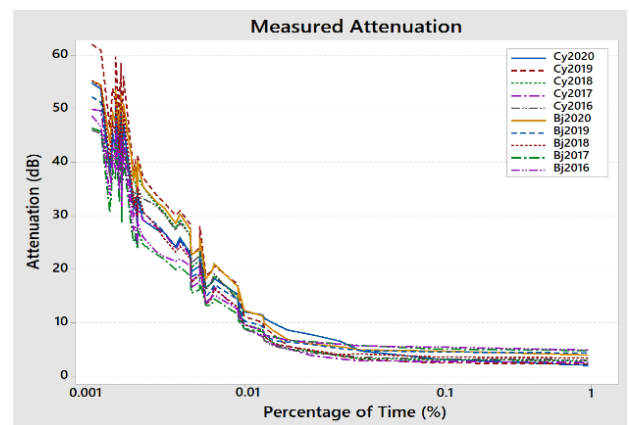


FIGURE 12. Measured attenuation from 2016 until 2020 for both Cy and Bj. until 2020 for both Cy and Bj.

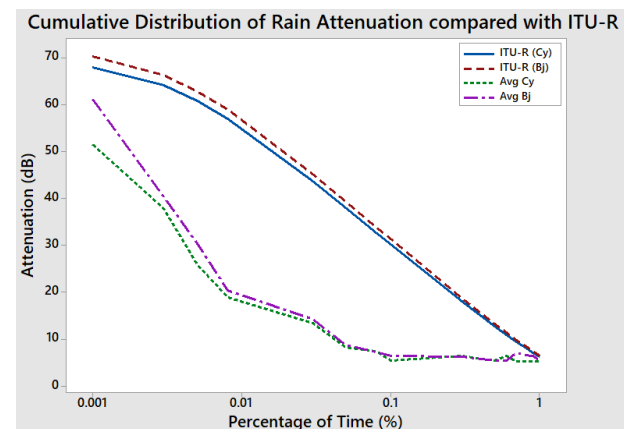


FIGURE 13. Comparison of measurement with attenuation ITU-R model.

recommendation from REC-P.618-13 [30] which presented in Figure 13. The root means square error (RMSE) is calculated and based on the comparison of the measured data and ITU recommendation.

To well capture the effect of the electrical bridge, the ERL are drive with a low speed of 12km/h. This is to ensure the result are more accurate (Figure 14) and observation found

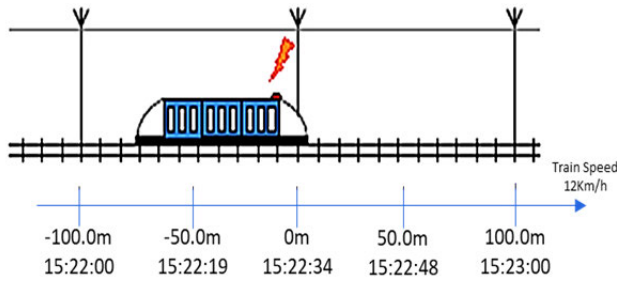


FIGURE 14. Electrical bridges and posts with time taken for analysis.

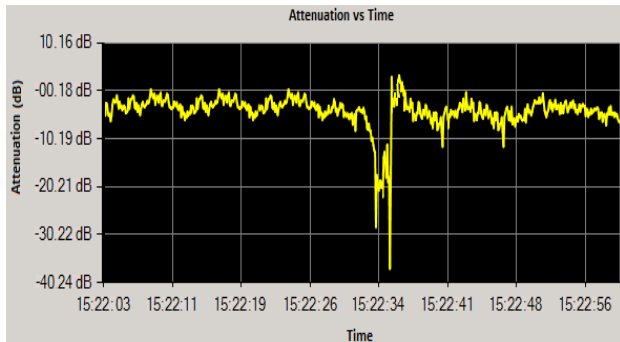


FIGURE 15. Attenuation due to an electrical bridge.

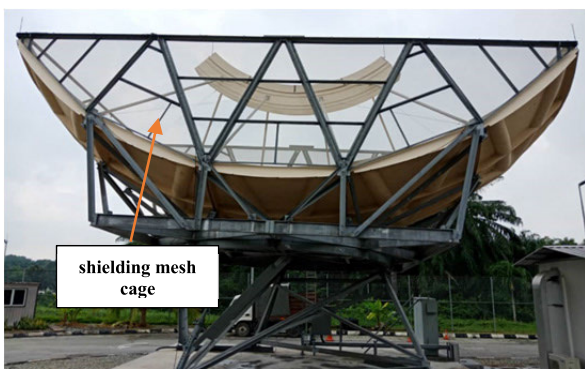


FIGURE 16. A shielding mesh cage installed at the simulast 7 (SS7) multibeam to avoid EMI interference.

that the packet loss is getting higher compare to the both of the previously analyzed scenario (Figure 9).

The EMI effect is clearly noticeable via spectrum analyser (SA) (Figure 15) which induce interference to the primary carrier of the transponder. This impact badly on the video and its QoS link availability on the user experience [29].

A faraday shielding mesh cage [30] (Figure 16 and 17) with specific dimension (using the equation of  $c = f \times \lambda$ ), where the  $c = 3 \times 10^8$  m / s,  $f =$  require operating frequency and  $\lambda$  represent the spacing of the mesh dimension based on specific frequency to be allowed which shields mainly target frequency.

It has suitable shielding effectiveness which weaken wireless communication in other unwanted frequency band with improved packet loss (Figure 18 and Figure 19 respectively). The comparison of carrier performance under the unshielded and shielded mesh were clearly noticeable via SA as shown



FIGURE 17. A shielding mesh cage installed on top of the array antenna which act as EMI radome.

in Figure 20. The efficient grounding is required to ensure no electric spark when the ERL are passing by catenaries [31]. This is to ensure proper safety mechanism conformity with EN-50155 compliance [32].

#### IV. RESULT AND DISCUSSION

The primary objective of the study is to provide a benchmark communication measurement between end-user equipment and power line emission including the atmospheric impairments under tropical region. Thus, a clear separation between power arch (PA) and other type of attenuation (i.e. rain, temperature) is require for a precise design of rail infotainment communication system. An earth terminal receiving signal elevation angle effect heavily to the communication performance. Which means, high elevation angle reduces the signal propagation path and rain attenuation [15].

Based on the Figure 10, the recorded attenuation is around 40 dB and as discussed [26] the rain attenuation plays a vital role under tropical region additional to the mobility impairment. Cyberjaya experience early outage on 2019 and 2020 at 0.01% of time reference towards the Figure 11 and Figure 12. The recorded average precipitation is at 172.39 mm/h and 157.44 mm/h respectively during Northeast Monsoon. This provide good analysis for designing communication system for OTM application in Malaysia region with the reference towards the rain pattern and attenuation level. Northeast Monsoon season (November to March) normally experience heavy rainfall and Feb 14th, 2020 been selected for the analysis due to maximum record rainfall. However, the ITU-R does not able to match the measured value (Figure 13) which it could possible due to the attenuation fading effect on the OTM antenna and further in-depth analysis is required.

Additionally, a reliable channel model validation can be formed based on the reference measured channel parameter as presented in Figure 10 with the changes of tropical rain pattern. Even a good signal strength could possibly provide a bad QoS due to the degradation of signal quality [35]. This can be seen on the packet loss result with a different of 18% recorded before and after the mesh installed. Ambient noise temperature might potentially affect the gain of receiving signal thus reduces the effective gain of the amplifier [36].

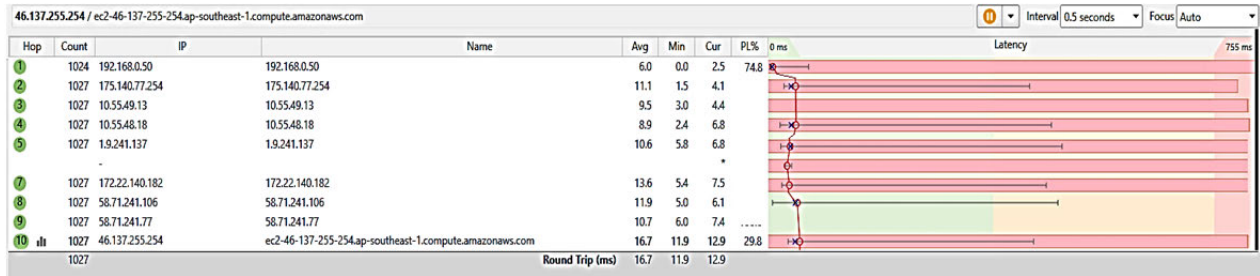


FIGURE 18. Packet loss result for the ERL during passing by the electric bridge before the shielding mesh cage installed.

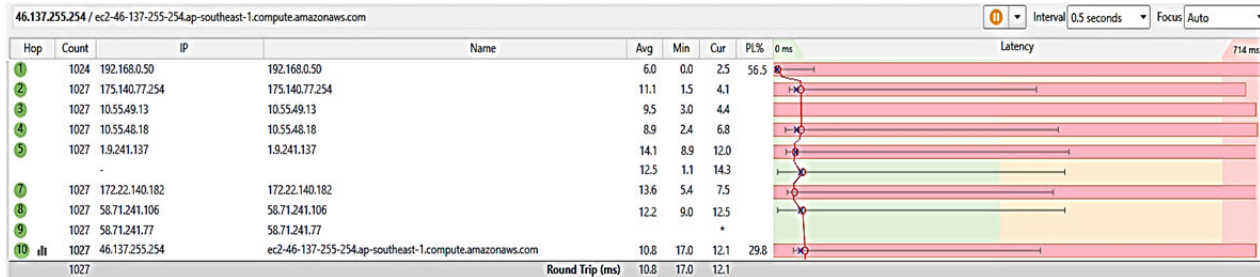


FIGURE 19. Packet loss result for the ERL during passing by the electric bridge after the shielding mesh cage installed.

TABLE 8. Percentage error analysis for both Cy and Bj with ITU-R model.

	Average Prediction		Average Measured		Cy	Bj
	ITU-R (Cy)	ITU-R (Bj)	Avg Cy	Avg Bj	$\epsilon(P)$	$\epsilon(P)$
0.001	67.92	70.11	51.42	61.03	0.32	0.15
0.003	64.09	66.23	37.82	40.27	0.69	0.64
0.005	60.71	62.77	25.77	30.27	1.36	1.07
0.008	56.87	58.82	18.75	20.36	2.03	1.89
0.03	43.57	45.12	13.26	14.21	2.29	2.18
0.05	37.91	39.28	8.11	8.65	3.67	3.54
0.08	32.64	33.83	7.41	7.25	3.40	3.67
0.1	30.13	31.25	5.37	6.35	4.62	3.92
0.3	18.03	18.72	6.36	6.24	1.84	2.00
0.5	12.66	13.16	5.32	5.37	1.38	1.45
0.6	10.83	11.26	6.36	5.37	0.70	1.10
0.7	9.34	9.71	5.24	6.97	0.78	0.39
0.8	8.10	8.43	5.27	6.44	0.54	0.31
0.9	7.05	7.34	5.16	6.36	0.37	0.16
1	6.16	6.42	5.24	5.33	0.18	0.20
				$\mu$	1.61	1.51
				$\sigma$	1.36	1.33
				RMS	2.11	2.01

So far, Railway Technical Research Institute (RTRI) and the National Institute of Information & Communication Technology (NICT) in Japan had carried out the measurement campaign at the satellite frequency above K-band [37].

TABLE 9. ERL communication performance.

Condition	ACM	Outbound throughput from remote location (Mbps)	Inbound throughput to remote location (Mbps)	Max Packet Loss (%)	Max Latency (ms)
Clear	16-APSK, 8/9	2.7648	45.6122	32.3	723
Rain	QPSK, 1/4	1.0240	6.0900	65.5	755

However, all the measurement campaigns focuses under the temperate region which the direct reference towards tropical region is inaccurate [38]. The available model such as Ali *et. al.* [6], Sujan *et. al.* [39] and Mandeep *et. al.* [40] are used to compare the actual measured channel performance with an average of 2.11 and 2.01 root mean square error (RMSE) for both Cyberjaya and Bukit Jalil respectively from ITU-R P.311-10 [26]. The detail RMSE result are presented in Table 8. As the near zero RMSE measurement are needed, more in-depth investigation of existing models and long term measured data is required.

Under the inbound link, this solution relies on the ACM DVB-S2/X standard, which characterizes mechanisms to guarantee a significant level of continuity with a Deep Packet Inspection (DPI) technology to limit the bandwidth usage based on the available throughput.

A network throughput (Table 9) is identified with maximum at a clear sky (16-APSK Rate 8/9 – 14.41 Mbps average per user) and minimum at rainy condition (QPSK Rate 1/4 – 2.41 Mbps average per user) before the signal completely attenuated [27]. An advance data processing application such as deep packet inspection is needed during the rainy condition. This will potentially reduce congestion during lower code rate (QPSK, 4) in managing overall network traffic.



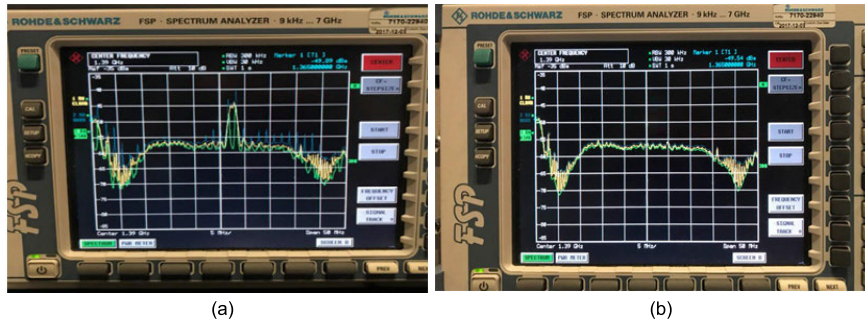


**FIGURE 20.** Carrier snapshot of spectrum analyser when ERL during passing by the electric bridge (a) without shielded mesh and (b) after shielded mesh installed.

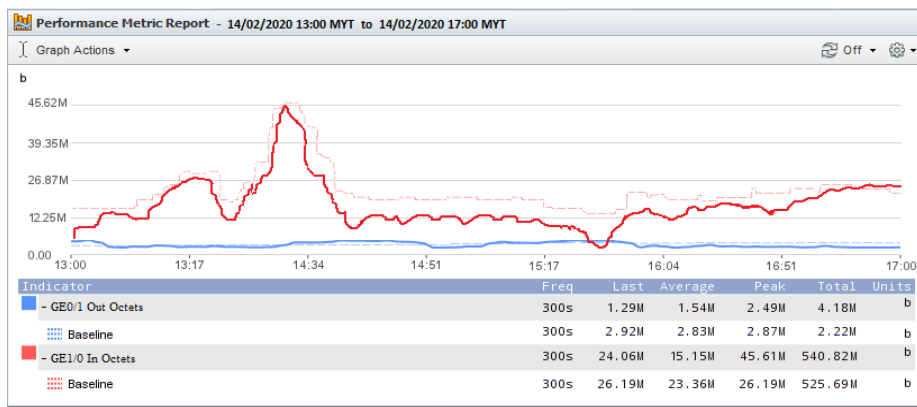


**FIGURE 21.** Average throughput per day during ERL in OTM on Feb 14<sup>th</sup>, 2020 with shielded mesh.

**TABLE 10.** Wireless network communication performance [33]–[35].

Technology	Data rate (Mbps)	Operating frequency (GHz)	Speed (km/h)
38G mmW (Maglev)	~ 8	37.1 ~ 38.5	< 500
Ku-Band (TGV)	~ 42	11	< 300
HTS Ka-Band (ERL)	~ 15	20.02	< 150
LTE (For common rail application)	~ 50	0.450 / 0.800 / 1.4	< 500
5G NR - FAST (Frequency Division Duplexing Assists Super Time Division Duplexing)	~ 1200 (up to 2Gbps)	2.1 & 3.5	< 500

As the indoor communication throughput is higher than the SatCom network, higher packet loss is observed (Figure 15). A reliable QoE and QoS as shared in Figure 21 with an average of 15Mbps can be achieved with a successive interference cancellation mechanism with a shielded mesh added to the receiver.

It is always a goal under the tropical region to achieve a throughput close to 5G NR wireless technology and an overall performance comparison available under the temperate region as summarised in Table 10. The most impportunity criteria for heterogonous SatCom LiFi solutions are: Availability for critical analytic applications, the packet loss and transfer delay between SatCom & LiFi remote terminals and customised throughput for multi-user handhelds devices.

**V. CONCLUSION AND FUTURE WORKS**

Heterogeneous Satcom-LiFi had entered next revolution long term potential solution under HTS for wireless communication. This investigation will provide useful information to system designer and analysts by understanding and considering the real environment of hybrid communication system network, predominantly in the tropical region, where such data is inadequate.

The comprehensive and well-planned measurement may introduce more precise hybrid network design mainly; (i) at OTM application, (ii) and at the policy-based orchestrator/controller layer. However, such executions will be expensive for researcher to reach the ideal requirement of the OTM communication network.

The main conclusions obtained are as follow:

- Reliability – Performance of the hybrid application
- Low latency – Immediate setup for cost avoidance is highly demanded in current era.
- Realtime analysis - Measurement under tropical geographical constraints and power arch performance examination.

Assuming that, the outbound teleport traffic are perfect, future works may include other available spectral efficiency scheme (proprietary of NovelSat®) for bandwidth efficient estimation techniques to further tweaking OTM service interruption.

## REFERENCES

- [1] T.-C. Chen, J.-H. Chiou, S.-W. Wei, and T.-T. Lin, "A handover algorithm for broadband wireless access system on railway," in *Proc. 2nd Int. Conf. Mech. Electron. Eng.*, Kyoto, Japam, 2010, pp. V1-98–V1-102.
- [2] Q. Fu, E. Sun, K. Meng, M. Li, and Y. Zhang, "Deep Q-learning for routing schemes in SDN-based data center networks," *IEEE Access*, vol. 8, pp. 103491–103499, 2020.
- [3] M. Leba, S. Riurean, and A. Lonica, "LiFi—The path to a new way of communication," in *Proc. 12th Iberian Conf. Inf. Syst. Technol. (CISTI)*, Lisbon, Portugal, Jun. 2017, pp. 1–6.
- [4] P. Pavarangkoon, K. T. Murata, M. Okada, K. Yamamoto, Y. Nagaya, T. Mizuhara, A. Takaki, K. Muranaga, and E. Kimura, "Bandwidth utilization enhancement using high-performance and flexible protocol for INTELSAT satellite network," in *Proc. IEEE 7th Annu. Inf. Technol., Electron. Mobile Commun. Conf. (IEMCON)*, Vancouver, BC, Canada, 2016, pp. 1–7.
- [5] A. H. J. Al-Jumaily, A. Sali, J. S. Mandeep, and A. Ismail, "Propagation models on Earth-sky signal effects for high speed train satellite channel in tropical region at Ku-band," *Int. J. Antennas Propag.*, vol. 2015, Feb. 2015, Art. no. 270949.
- [6] A. M. Al-Saegh, A. Sali, J. S. Mandeep, and F. P. Fontán, "Channel measurements, characterization, and modeling for land mobile satellite terminals in tropical regions at Ku-band," *IEEE Trans. Veh. Technol.*, vol. 66, no. 2, pp. 897–911, Feb. 2017.
- [7] D. Wu, P. Ho, J. Chen, J. Yang, and H. Chang, "Signal measurement and prediction of WiMAX basestations on Taiwan high speed rail," in *Proc. IEEE Int. Conf. Consum. Electron.-Taiwan (ICCE-TW)*, Nantou, Taiwan, Oct. 2016, pp. 1–2, doi: [10.1109/ICCE-TW.2016.7520946](https://doi.org/10.1109/ICCE-TW.2016.7520946).
- [8] L. Ma, "Satellite-terrestrial channel characterization in high-speed railway environment at 22.6 GHz," *Radio Sci.*, vol. 55, no. 3, pp. 1–15, Mar. 2020, doi: [10.1029/2019RS006995](https://doi.org/10.1029/2019RS006995).
- [9] K. Guan, B. Peng, D. He, J. M. Eckhardt, S. Rey, B. Ai, Z. Zhong, and T. Kürner, "Channel characterization for intra-wagon communication at 60 and 300 GHz bands," *IEEE Trans. Veh. Technol.*, vol. 68, no. 6, pp. 5193–5207, Jun. 2019, doi: [10.1109/TVT.2019.2907606](https://doi.org/10.1109/TVT.2019.2907606).
- [10] C. Wu, X. Cai, J. Sheng, Z. Tang, B. Ai, and Y. Wang, "Parameter adaptation and situation awareness of LTE-R handover for high-speed railway communication," *IEEE Trans. Intell. Transp. Syst.*, early access, Oct. 6, 2020, doi: [10.1109/TITS.2020.3026195](https://doi.org/10.1109/TITS.2020.3026195).
- [11] X. Zhang, N. Li, W. Zhu, and D. K. Sung, "TCP transmission rate control mechanism based on channel utilization and contention ratio in ad-hoc networks," *IEEE Commun. Lett.*, vol. 13, no. 4, pp. 280–282, Apr. 2009.
- [12] S. Islam, N. Muslim, and J. W. Atwood, "A survey on multicasting in software-defined networking," in *IEEE Commun. Surveys Tuts.*, vol. 20, no. 1, pp. 355–387, 1st Quart., 2018.
- [13] L. U. Khan, "Visible light communication: Applications architecture standardization and research challenges," *Digit. Commun. Netw.*, vol. 3, no. 2, pp. 78–88, May 2017.
- [14] W. Xu, H. A. Omar, W. Zhuang, and X. S. Shen, "Delay analysis of in-vehicle Internet access via on-road WiFi access points," *IEEE Access*, vol. 5, pp. 2736–2746, 2017.
- [15] *Radiation Diagrams for Use as Design Objectives for Antennas of Earth Stations Operating With Geostationary Satellites*, document ITU-R S.580, International Telecommunication Union, Geneva, Switzerland, 2001.
- [16] J. M. Inclán-Alonso, A. García-Aguilar, L. Vigil-Herrero, J. M. Fernández-González, J. SanMartín-Jara, and M. Sierra-Pérez, "Portable low-profile antenna at X-band," in *Proc. 5th Eur. Conf. Antennas Propag. (EUCAP)*, Rome, Italy, 2011, pp. 1923–1927.
- [17] D. Duyck, M. Mertens, J. Vandendruaene, D. Breynaert, and F. Simoens, "An efficiency comparison between timeslicing and multi-carrier transmission for linearized transponders," in *Proc. 36th Int. Commun. Satell. Syst. Conf. (ICSSC)*, Niagara Falls, ON, Canada, 2018, pp. 1–5.
- [18] D. Duyck, A. Mengali, M. B. Shankar, K. Liolis, C. Le Guern, B. T. Jou, and S. Cioni, "An overview of multicarrier predistortion techniques and associated throughput gain for an actual hardware implementation," in *Proc. AIAA Intern. Comm. Sat. Systems Conf. (ICSSC)*, Oct. 2017, pp. 352–362.
- [19] N. P. Pathak, A. Basu, S. K. Koul, and B. Bhat, "Numerical and experimental analysis of nonradiative dielectric guide modulator and mixer at Ka-band," *IEEE Microw. Wireless Compon. Lett.*, vol. 14, no. 7, pp. 322–324, Jul. 2004.
- [20] *Malaysia Express Rail Link Technical Report*. Accessed: 2013. [Online]. Available: <https://www.kliaekspres.com/wp-content/uploads/2013/01>
- [21] M. Kassim, R. A. Rahman, M. A. A. Aziz, A. Idris, and M. I. Yusof, "Performance analysis of VoIP over 3G and 4G LTE network," in *Proc. Int. Conf. Electr., Electron. Syst. Eng. (ICEESE)*, Kanazawa, Japan, 2017, pp. 37–41.
- [22] P. M. Kalaivaanan, A. Sali, R. S. A. R. Abdullah, S. Yaakob, M. J. Singh, and A. M. Al-Saegh, "Measuring contention and congestion on ad-hoc multicast network towards satellite on Ka-band and LiFi communication under tropical environment region," *IEEE Access*, vol. 8, pp. 108942–108951, 2020.
- [23] P.-C. Lin, Y.-D. Lin, T.-H. Lee, and Y.-C. Lai, "Using string matching for deep packet inspection," *IEEE Comput. Soc.*, vol. 41, no. 4, pp. 23–28, Apr. 2008.
- [24] S. Yadav, P. Mishra, M. Velapure, and P. P. S. Togrikar, "Li-Fi: Data transmission through illumination," *Int. J. Sci. Eng. Res.*, vol. 6, pp. 1432–1436, Oct. 2016.
- [25] A. Gomez, K. Shi, and C. Quintana, "Beyond 100-Gb/s indoor wide field-of-view optical wireless communications," *IEEE Photon. Technol. Lett.*, vol. 27, no. 4, pp. 367–370, Feb. 15, 2015.
- [26] P. M. Kalaivaanan, A. Sali, R. S. A. Raja Abdullah, S. Yaakob, M. Jit Singh, and A. M. Al-Saegh, "Evaluation of Ka-band rain attenuation for satellite communication in tropical regions through a measurement of multiple antenna sizes," *IEEE Access*, vol. 8, pp. 18007–18018, 2020.
- [27] S. D. Awad, A. Sali, A. M. Al-Saegh, M. M. Al-Wani, R. S. A. R. Abdullah, and J. S. Mandeep, "Beamforming and scheduling techniques for multi-beam DVB-S2X over rainy fading satellite channel," *IEEE Access*, vol. 1, no. 8, pp. 41116–41127, Dec. 2020.
- [28] A. M. Al-Saegh and T. A. Elwi, "Direct extraction of rain-induced impairments on satellite communication channel in subtropical climate at K and Ka bands," *Telecommun. Syst.*, vol. 74, pp. 15–25, Oct. 2020.
- [29] S. L. Jong, H. Y. Lam, J. Din, and M. D. Amico, "Investigation of Ka-band satellite communication propagation in equatorial regions," *ARPN J. Eng. Appl. Sci.*, vol. 10, no. 20, pp. 9795–9799, 2013.
- [30] G. Göcse, B. Németh, Z. Tamus, I. Kiss, and J. Meixner, "Shielding efficiency of conductive clothing during live-line maintenance," in *Proc. 11th Int. Conf. Live Maintenance (ICOLIM)*, Budapest, Hungary, 2014, pp. 1–5.
- [31] A. Morant, Å. Wisten, D. Galar, U. Kumar, and S. Niska, "Railway EMI impact on train operation and environment," *Int. Symp. Electromagn. Compat.*, Rome, Italy, 2012, pp. 1–7.
- [32] *Railway Application—Railway Rolling Stock in General*, document IEC/TC9-IEC\_TC\_9SIST 50153:2014/A2, 2020.
- [33] S. Cioni, C. P. Niebla, G. S. Granados, S. Scalise, A. Vanelli Coralli, and M. A. V. Castro, "Advanced fade countermeasures for DVB-S2 systems in railway scenarios," *EURASIP J. Wireless Commun. Netw.*, vol. 2007, Oct. 2007, Art. no. 49718.
- [34] J. Talvitie, T. Levanen, M. Koivisto, K. Pajukoski, M. Renfors, and M. Valkama, "Positioning of high-speed trains using 5G new radio synchronization signals," in *Proc. IEEE Wireless Commun. Netw. Conf. (WCNC)*, Barcelona, Spain, 2018, pp. 1–6.
- [35] F. Hasegawa, "High-speed train communications standardization in 3GPP 5G NR," *IEEE Commun. Standards Mag.*, vol. 2, no. 1, pp. 44–52, Mar. 2018.
- [36] C. Osborne and V. Rodriguez, "A method for gain over Temperature measurements using two 'hot' noise sources," in *Proc. 10th Eur. Conf. Antennas Propag. (EuCAP)*, Davos, Switzerland, 2016, pp. 1–5, doi: [10.1109/EuCAP.2016.7481286](https://doi.org/10.1109/EuCAP.2016.7481286).

- [37] K. Guan, B. Ai, B. Peng, D. He, G. Li, and J. Yang, "Towards realistic high-speed train channels at 5G millimeter-wave band—Part II: Case study for paradigm implementation," *IEEE Trans. Veh. Technol.*, vol. 67, no. 10, pp. 9129–9144, Oct. 2018.
- [38] K. Ulaganathan, T. A. Rahman, M. R. Islam, and N. A. Malek, "Mitigation technique for rain fade using frequency diversity method," in *Proc. IEEE 12th Malaysia Int. Conf. Commun. (MICC)*, Kuching, China, Apr. 2015, pp. 82–86.
- [39] S. Shrestha and D.-Y. Choi, "Study of rain attenuation in Ka-band for satellite communication in South Korea," *J. Atmos. Solar-Terr. Phys.*, vol. 148, pp. 53–63, Oct. 2016.
- [40] J. S. Mandeep, R. Nalinggam, and W. B. Ismail, "Analysis of rain attenuation models for south east Asia countries," *J. Infrared, Millim. THz Waves*, vol. 32, no. 2, pp. 233–240, 2011.
- [41] C. Chen, B.-L. Liu, L. Ji, and W.-D. Chen, "A high-isolation dual-polarization substrate-integrated Fabry–Pérot cavity antenna," *Int. J. Antennas Propag.*, vol. 2015, Jun. 2015, Art. no. 265962.
- [42] Y. Wang and A. M. Abbosh, "Software-defined reconfigurable antenna using slotted substrate integrated waveguide for Ka-band satellite-on-the-move communication," in *Proc. Int. Symp. Antennas Propag. (ISAP)*, Hobart, NSW, Australia, 2015, pp. 1–3.
- [43] S. M. R. Islam, D. Kwak, H. Kabir, M. Hossain, and K.-S. Kwak, "The Internet of Things for health care: A comprehensive survey," *IEEE Access*, vol. 3, pp. 678–708, Oct. 2015.
- [44] E. Abass, J. Halim, and H. El-Hennawy, "Performance assessment of coded-beam high throughput satellites," *Int. J. Commun., Netw. Syst. Sci.*, 10, pp. 218–226, Oct. 2017.
- [45] Q. Xu, H. Ji, X. Li, and H. Zhang, "Admission control scheme for service dropping performance improvement in high-speed railway communication systems," *IEEE Trans. Veh. Technol.*, vol. 65, no. 7, pp. 5251–5263, Jul. 2016.
- [46] N. Soumyalatha, R. K. Ambhati, and M. R. Kounte, "Performance evaluation of ip wireless networks using two-way active measurement protocol," in *Proc. Int. Conf. Adv. Comput., Commun. Informat. (ICACCI)*, Mysore, India, 2013, pp. 1896–1901.
- [47] U. Murat, C. Caponi, Z. Ghassemlooy, A. Boucouvalas, and E. Udvary, *Optical Wireless Communications an Emerging Technology*. Cham, Switzerland: Springer, 2016.
- [48] A. Balador and A. Movaghar, "The novel contention window control scheme for IEEE 802.11 Mac protocol," in *Proc. 2nd Int. Conf. Netw. Secur., Wireless Commun. Trusted Comput.*, Wuhan, China, 2010, pp. 134–137.
- [49] S. Rajagopal, R. D. Roberts, and S.-K. Lim, "IEEE 802.15.7 visible light communication: Modulation schemes and dimming support," *IEEE Commun. Mag.*, vol. 50, no. 3, pp. 72–82, Mar. 2012.
- [50] S. Kunniyur and R. Srikant, "End-to-end congestion control schemes: Utility functions, random losses and ecn marks," in *Proc. IEEE INFOCOMM*, vol. 3, Mar. 2000, pp. 1323–1332.
- [51] L. I. Albraheem, L. H. Alhudaithy, A. A. Aljaser, M. R. Aldhafian, and G. M. Bahliwah, "Toward designing a Li-Fi-based hierarchical IoT architecture," *IEEE Access*, vol. 6, pp. 40811–40825, 2018.
- [52] E. Hamadani and V. Rakocevic, "TCP contention control: A cross-layer approach to improve TCP performance in multihop ad hoc networks," in *Proc. 5th Int. Conf. Wired/Wireless Internet Commun.*, 2007, pp. 1–7.
- [53] C. Mala and B. Nithya, "Dynamic sliding contention window adjustment in saturated wireless networks," in *Proc. 17th Int. Conf. Netw.-Based Inf. Syst., Saler*, 2014, pp. 186–193.
- [54] A. Fantinato, N. Conci, T. Rossi, and C. Sacchi, "Performance analysis of W-band satellite HDTV broadcasting," in *Proc. Aerosp. Conf.*, Big Sky, MT, USA, 2011, pp. 1–12.
- [55] C. Yang, M. Liao, M. Luo, S. Wang, and C. E. Yeh, "A network management system based on DPI," in *Proc. 13th Int. Conf. Netw.-Based Inf. Syst.*, Takayama, Japan, 2010, pp. 385–388.
- [56] S. Gong, D. Wei, X. Xue, and M. Y. Chen, "Study on the channel model and BER performance of single-polarization satellite-Earth MIMO communication systems at Ka-band," *IEEE Trans. Antennas Propag.*, vol. 62, no. 10, pp. 5282–5297, Oct. 2014.
- [57] N. Kiji, T. Sato, R. Shinkuma, and E. Oki, "Virtual network function placement and routing for multicast service chaining using merged paths," *Opt. Switching Netw.* vol. 36, Feb. 2020, Art. no. 100554.
- [58] O. Kodheli, "Satellite communications in the new space era: A survey and future challenges," *IEEE Commun. Surveys Tuts.*, vol. 23, no. 1, pp. 70–109, 4th Quart., 2021, doi: 10.1109/COMST.2020.3028247.
- [59] *DVB Technical Report Over Broadband Satellite*. Accessed: 2005. [Online]. Available: [https://www.etsi.org/deliver/etsi\\_en/302300302399/30230702/01.01.01\\_20/en\\_30230702v010101a.pdf](https://www.etsi.org/deliver/etsi_en/302300302399/30230702/01.01.01_20/en_30230702v010101a.pdf)
- [60] *DVB Technical Report Over Broadband Satellite*. Accessed: 2014. [Online]. Available: [https://www.etsi.org/deliver/etsi\\_en/302300\\_302399/30230701/01.04.01\\_60/en\\_30230701v010401p.pdf](https://www.etsi.org/deliver/etsi_en/302300_302399/30230701/01.04.01_60/en_30230701v010401p.pdf)
- [61] M. Torrent-Moreno, J. Mittag, P. Santi, and H. Hartenstein, "Vehicle-to-vehicle communication: Fair transmit power control for safety-critical information," *IEEE Trans. Veh. Technol.*, vol. 58, no. 7, pp. 3684–3703, Sep. 2009.
- [62] G. Berretta, P. Dvorak, M. Luglio, L. Luini, C. Riva, C. Roseti, and F. Zampognaro, "Improvement of Ka-band satellite link availability for real-time IP-based video contribution," *ICT Exp.*, vol. 3, no. 3, pp. 124–127, 2017.
- [63] F. Samat and M. S. Jit Singh, "Impact of rain attenuation to Ka-band signal propagation in tropical region: A study of 5-year MEASAT-5's beacon measurement data," *Wireless Pers Commun*, vol. 112, pp. 2725–2740, May 2020.



**P. M. KALAIVAANAN** (Graduate Student Member, IEEE) received the B.Eng. degree in communication engineering from University Malaysia Perlis, in 2007, and the master's degree in engineering management from University Putra Malaysia (UPM), in 2016, where he is currently pursuing the Ph.D. degree in communication and network engineering. He is also a Postdoctoral Researcher with the Faculty of Engineering, UPM. His research interests include satellite communication and visible light communication (VLC).



**ADUWATI SALI** (Senior Member, IEEE) received the B.Eng. degree in electrical electronics engineering (communications) from The University of Edinburgh, U.K., in 1999, the M.Sc. degree in communications and network engineering from Universiti Putra Malaysia (UPM), Malaysia, in April 2002, and the Ph.D. degree in mobile and satellite communications from the University of Surrey, U.K., in July 2009. She has been a Professor with the Department of Computer and Communication Systems, Faculty of Engineering, UPM, since February 2019. She was the Deputy Director of the UPM Research Management Centre (RMC) and is responsible for research planning and knowledge management. She worked as an Assistant Manager with Telekom Malaysia Bhd., from 1999 until 2000. She is currently a Chartered Engineer (C.Eng.) registered under the U.K. Engineering Council and a Professional Engineer (P.Eng.) under the Board of Engineers Malaysia (BEM). Her research interests include radio resource management, MAC layer protocols, satellite communications, satellite-assisted emergency communications, the IoT systems for environmental monitoring, and 3D video transmission over wireless networks. She was involved with IEEE as a Chairperson to Com-Soc/VTS Malaysia, from 2017 to 2018, Young Professionals (YP) (2015; Young Scientists Network-Academy of Sciences Malaysia (YSN-ASM) as the Chair, in 2018, and the Co-Chair, in 2017, for Science Policy. She is also the Principal Investigator and a Collaborator in projects under local and international funding bodies, namely, Malaysian Ministry of Science, Technology and Innovation (MOSTI), Malaysian Ministry of Higher Education (MoHE), Malaysian Communications and Multimedia Commission (MCMC), Research University Grant Scheme (RUGS) (now known as Putra Initiative Grant), UPM, the Academy of Sciences for the Developing World (TWAS-COMSTech) Joint Grants, the EU Horizon 2020 Research and Innovation Staff Exchange (H2020-RISE), and the NICT Japan-ASEAN IVO. She provided consultation to the Malaysian Ministry of Information and Multimedia, Malaysian Ministry of Higher Education, National Space Agency (ANGKASA), ATSB Bhd., and Petronas Bhd. on projects related to mobile and satellite communications. In 2014, due to the fateful disappearance of MH370, she appeared in printed and broadcasting media, specifically Astro Awani, RTM, TV Al-Hijrah, BERNAMA, Harian Metro, and Metro Ahad, regarding the analysis of satellite communication in tracking the missing aircraft.



**RAJA SYAMSUL AZMIR RAJA ABDULLAH** (Senior Member, IEEE) received the B.Eng. degree in electronic and electrical engineering and the M.Sc. degrees in communication system engineering from the University of Birmingham, U.K., in 2000 and 2001, respectively, and the Ph.D. degree from the University of Birmingham majoring in radar and microwave systems. His research interests include microwave systems, radar systems, and wireless sensor networks, and he has

been involved in the development of hardware and software for radar sensors and wireless sensor networks (WSNs). He has contributed to the development of the advanced practical forward scattering radar (FSR) systems; and the system has been adopted for various applications, including civil, military, and medical. With the addition of an intelligent system, the advanced FSR system can automatically detect and classify most ground and air targets. Recent development focuses on the high-resolution radar network (RSN), which can be applied to small-object detection and classification. By adopting WSN advantages, the drawbacks of traditional radar can be compensated. Future radar will have the size of a computer mouse compared with the huge radar set mounted on towers at present. He is also the IEEE graduate of the last decade (Young Professional), Malaysia, in 2008, a member, IEEE Aerospace and Electronic System, Society, an Executive Member, the IEEE graduate of the last decade, Malaysia, in 2007, a member European microwave association, in 2007, and a member of the Malaysian Society for Engineering and Technology, since 2008, the International Association of Engineers (IAENG), since 2008, and the Institution of Engineering and Technology (IET), since 2002.



**SYAMSURI YAAKOB** (Senior Member, IEEE) received the B.Eng. degree in electronic engineering from King's College London, in 1998, the M.Eng.Sc. degree in electronic engineering from Multimedia University (MMU), Cyberjaya, in 2010, and the Ph.D. degree in millimetre-wave radio over fibre system from Universiti Teknologi Malaysia (UTM), in 2014. He is currently an Associate Professor with the Department of Computer and Communication Systems Engineering,

Faculty of Engineering, Universiti Putra Malaysia (UPM). Prior to this appointment, he was a Satellite Engineer with Telekom Malaysia, in 1998, and a Senior Researcher with TM Research and Development Sdn. Bhd. (TMR&D), in 2004. His current research interests include millimetre-wave radio over fibre systems, passive optical networks, optical communication systems, and access network technologies.



**MANDEEP JIT SINGH** was born in Malaysia, in 1975. He is currently a Professor with the Department of Electrical, Electronic and Systems Engineering, Universiti Kebangsaan Malaysia (UKM), and a Visiting Professor with Covenant University, Nigeria. He is also the Advisor of the Engineering Education Technical Division (E2TD), Institute of Engineers, Malaysia. He is the author and coauthor of more than 240 research articles in antenna and microwave RF. He was a

recipient of more than 40 research grants (national and international). Thus far, his publications have been cited 959 times, and his H-index is 15. His research interests include communication antenna design, radio wave propagation, satellite antennas, and the IoT. He received several international and national medal awards for his research and innovation. He also serves as the Editor-in-Chief for the *Greener Journal of Electronics* and the *Communication* and an Associate Editor for the *Journal of Electrical and Computer Engineering* (Hindawi).



**ALI M. AL-SAEGH** was born in Baghdad, Iraq, in April 1984. He received the B.Sc. degree in electronic and communications engineering from Nahrain University, Iraq, in 2005, the M.Sc. degree in satellite engineering from the Electronic and Communications Engineering Department, Nahrain University, in 2008, and the Ph.D. degree in wireless communications engineering from the Computer and Communication System Engineering Department, Universiti Putra Malaysia (UPM),

Malaysia, in 2015. From 2009 to 2012, he has served as a Lecturer for the Computer Engineering Techniques Department and the Communications Engineering Department, Al-Ma'moon University College, Iraq. From 2012 to 2013, he worked as a Research Assistant with the Department of Computer and Communication Systems Engineering, UPM. Since 2015, he has been a Senior Lecturer with the Computer Engineering Techniques Department, Al-Ma'moon University College. His research interests include radiowave propagation, satellite communications, atmospheric impairment prediction, channel modeling, multimedia transmission, and resource management. He is also a member of several groups and associations, including the satellite communications group in UPM, Malaysia, Iraqi engineering and academic associations, and several IEEE societies and communities.

• • •